Received March 2004
Revised November 2004
Accepted February 2005

Temperature dependent fluid properties effects on the heat function formulation of natural convective flow and heat transfer

M. Adekojo Waheed
Mechanical Engineering Department, Ladoke Akintola University of Technology, Ogbomoso, Nigeria

Abstract

Purpose – To study quantitatively the effects of combined temperature dependent thermodynamics and transport fluid properties on the heat transfer rate, heat function fields and profiles in a fluid filled square enclosure.

Design/methodology/approach – Navier-Stokes equations in two-dimensions, which are the flow governing equations, were transformed into stream function and vorticity transport equations. These equations together with the energy and heat function equations were cast into their non-dimensional forms. Numerical solutions of the resulting equations were done by the use of finite-difference method.

Findings – The numerical investigations conducted covered the Rayleigh and Prandtl numbers in the range $10^3 \leq Ra \leq 10^6$ and $0.01 \leq Pr \leq 450$, respectively, and expansion parameter $\varepsilon = (T_h - T_c)/T_R$ in the range $0.05 \leq \varepsilon \leq 1$. Results show that Boussinesq-approximation is not sufficient to simulate natural convective flow when the difference between T_h and T_c is high and close to the reference state temperature. The effects of the other fluids properties other than density can be disregarded in computation without significant loss of accuracy. Combined fluid properties have very strong effects on the heat transfer, heat function fields and profiles.

Originality/value – The results of this study will serve as baseline information to designers of heat transfer or process equipment in which fluid at very high temperature occurs.

Keywords Fluids, Convection, Heat transfer

Paper type Research paper

Nomenclature

c_p = specific heat capacity of fluid (J/kg K)
g = acceleration due to gravity (m/s^2)
Ga = Galilei number
Gr = Grashof number
h = enclosure height (m)
H = heat function (W/m)
J = ratio of T_R and $(T_h - T_c)$
l = enclosure length (m)
M = number of vertical grid lines
N = number of horizontal grid lines
Nu = Nusselt number, $Q/\lambda\Delta T$
p = pressure (N/m^2)
Pr = Prandtl number
Q = overall heat transfer rate (W)
Ra = Rayleigh number
T = temperature (K)
u = horizontal velocity (m/s)
v = vertical velocity (m/s)
x = horizontal coordinate (m)
y = vertical coordinate (m)

Abbreviations
BA = Boussinesq-approximation
VFP = variable fluid properties

Greek alphabet
α = fluid thermal diffusivity (m^2/s)
β = volumetric coefficient of thermal expansion (/K)
ε = expansion parameter

International Journal of Numerical Methods for Heat & Fluid Flow
Vol. 16 No. 2, 2006
pp. 240-260

0961-5539
DOI 10.1108/09615530610644299

λ = thermal conductivity of fluid (W/m K)
μ = viscosity (Pa s)
υ = kinematic viscosity (m^2/s)
ρ = density (kg/m^3)
ψ = stream function (m^2/s)
ω = vorticity (m/s)
Ω = relaxation factor
ϕ = primary variable

Sub- and superscripts
c = cold wall
h = hot wall
R = reference state condition
* = variables in their raw forms
n = computation step

1. Introduction

Natural convective flow and heat transfer had been intensively investigated in the past few decades by many researchers. This is due largely to its direct relevance in a variety of applications in nature and in engineering practices, ranging from growth of crystals, solar collection performance, fire and smokes spread in rooms and compartments to large-scale geophysical phenomena. The investigations had been carried out theoretically (Cormack *et al.*, 1974), numerically (De Vahl Davis, 1983; Miyamoto *et al.*, 1989; Chen *et al.*, 1990; Kelkar and Patankar, 1990; Lee, 1999; Mota *et al.*, 2000) and experimentally (Inaba and Fukuda, 1984; Ivey and Hamblin, 1989). The basis for the numerical investigation is the solution of the complete Navier-Stokes and the energy equations. It was assumed in all the numerical computations of natural convection that all the fluid properties are constant except for the density changes with temperature in the buoyancy term of the equation of motion. This assumption leads to the so-called Boussineq-approximation. The approximation is the almost universally adopted method in the theoretical calculations of natural convection. But this approximation is valid for small temperature differences only (Zhong *et al.*, 1985).

The investigation of heat transfer by natural convection rests on the premise that on one side the approximation gives good results for some definite areas. On the other side, the solution of the complete equations with variable fluid properties is inhibited by the computer capacity and the available numerical methods. But the complete Navier-Stokes equations are not only connected through the density with the energy equation, but also through the temperature dependent transport properties such as viscosity, thermal conductivity and specific heat capacity. The transport properties for liquids vary appreciably for a small change in temperature. For example, the dynamic viscosity of water reduces by about 50 per cent for a temperature rise from 10 to 40°C (Thielemann, 1985; De Souza *et al.*, 2003). The dynamic viscosity of oils is essentially strongly temperature dependent. Thielemann (1985) stated that by high temperature difference, there is a significant deviation of heat transfer and especially of the flow pattern of the Boussineq-approximation from the solution of variable fluid properties. Merker and Mey (1987) and Hong (1992) investigated natural convection in flat rectangular enclosures filled with air, oil or water. The effects of temperature dependent fluid properties were thereby considered. They hinted that the choice of the reference temperature plays an important role on the flow pattern when variable fluid properties are considered as compared with the results for Boussineq-approximation. The focus of attention in these works was on the study of the effects of Rayleigh number, Prandtl number, aspect ratio and the cavity inclination angles on the flow patterns, isotherms, and on the convective heat transfer. Isotherm was, however,

adjudged not to give good representation of the energy field in convection dominated fields (Hong, 1992).

Kimura and Bejan (1983) proposed the use of heatlines for the visualization of the heat transfer by convection. They tested their proposed heat function model to visualize convective heat transfer in a rectangular enclosures bounded by two isothermal vertical and two adiabatic horizontal walls. Bello-Ochende (1986, 1988) extended the pioneering work of Kimura and Bejan by adding a vortex term to the heat function model, which was supposedly omitted by the pioneers. Besides these two known work on heat function and a small account by Griebel *et al.* (1998), there is no known comprehensive work on the subject matter. The effects of variation of the fluid properties on heat function and thus on energy trajectory in convective field have not been considered to date.

The purpose of this work is therefore to investigate the effects of temperature dependent fluid properties, namely density, viscosity, thermal conductivity and specific heat capacity on free convection and heat function. The effects of Rayleigh and Prandtl numbers on energy trajectory are thereby investigated.

2. The physical system and the mathematical models

Figure 1 shows a schematic diagram of a two-dimensional enclosure used in this study for the investigation of the effects of variable fluid properties on the energy trajectory in convective flow fields. This configuration together with the prescribed boundary conditions is used to describe a classical problem for the study of free convective flow in rectangular enclosure (Kimura and Bejan, 1983). In this configuration, the enclosure is conceived such that it is bounded by two end walls that are held at constant but different temperatures, T_h and T_c, $T_h > T_c$, and by the lower and the upper walls that are adiabatic. The dimension of the cavity is infinitesimally long in the z-direction so that only velocity and temperature changes in the plane need to be computed.

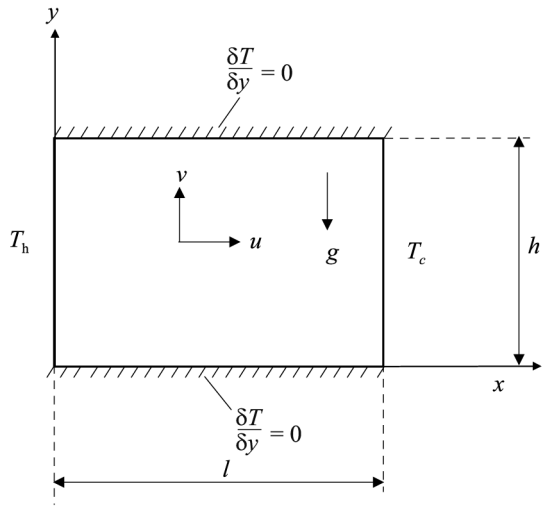

Figure 1.
The definition of control field with the normalized boundary constraints and the coordinate axes

The gravitational force acts in a direction opposite the y-axis. The flow is assumed laminar and stationary, and the fluid Newtonian.

The fundamental equations for the mathematical description of the free convective flow are the continuity, Navier-Stokes and energy equations. These equations are respective expressions for conservation of mass, momentum and energy. Thielemann (1985) stated that the dissipation energy and the pressure term in the energy equation are very small in comparison with other terms. These are thus neglected in this work. The basic equations for two-dimensional steady flow in Cartesian coordinates can be written as follows (Schlichting and Gersten, 2000).

The equation of continuity:

$$\frac{\partial \rho^* u^*}{\partial x^*} + \frac{\partial \rho^* v^*}{\partial y^*} = 0 \tag{1}$$

The equation of motion in the x- and y-directions:

$$\rho^* \left(u^* \frac{\partial u^*}{\partial x^*} + v^* \frac{\partial u^*}{\partial y^*} \right) = - \frac{\partial p^*}{\partial x^*} + \left(\frac{\partial \tau_{xx}}{\partial x^*} + \frac{\partial \tau_{yx}}{\partial y^*} \right) \tag{2}$$

$$\rho^* \left(u^* \frac{\partial v^*}{\partial x^*} + v^* \frac{\partial v^*}{\partial y^*} \right) = - \frac{\partial p^*}{\partial y^*} - \rho^* g + \left(\frac{\partial \tau_{xy}}{\partial x^*} + \frac{\partial \tau_{yy}}{\partial y^*} \right) \tag{3}$$

with

$$\tau_{xx} = \mu^* \left(2 \frac{\partial u^*}{\partial x^*} - \frac{2}{3} \left(\frac{\partial u^*}{\partial x^*} + \frac{\partial v^*}{\partial y^*} \right) \right)$$

$$\tau_{yy} = \mu^* \left(2 \frac{\partial v^*}{\partial y^*} - \frac{2}{3} \left(\frac{\partial u^*}{\partial x^*} + \frac{\partial v^*}{\partial y^*} \right) \right)$$

$$\tau_{xy} = \tau_{yx} = \mu^* \left(\frac{\partial u^*}{\partial y^*} + \frac{\partial v^*}{\partial x^*} \right)$$

The thermal energy equation:

$$u^* \frac{\partial T^*}{\partial x^*} + v^* \frac{\partial T^*}{\partial y^*} = \frac{1}{\rho^* c_p^*} \left(\frac{\partial}{\partial x^*} \left(\lambda^* \frac{\partial T^*}{\partial x^*} \right) + \frac{\partial}{\partial y^*} \left(\lambda^* \frac{\partial T^*}{\partial y^*} \right) \right) \tag{4}$$

The variables u^*, v^*, p^*, ρ^* and T^* are the fluid velocity components in the x^*- and y^*-directions, pressure, density, and temperature, respectively. The parameter λ^*, μ^* and g are, respectively, the coefficient of thermal conductivity, dynamic viscosity and gravitational acceleration.

Kimura and Bejan adjudged the use of heatlines for the visualization of the energy trajectory as standard. A heatline describes the course of heat energy in a flowing fluid as given by a line of constant heat function. The function is described such that the net flow of energy by thermal diffusion and enthalpy vanishes across a line of constant

heat function. Consequently, the level curves of heat function run parallel to the local heat flux.

Heat function is defined for the net heat transport in the x^*-direction as:

$$\frac{\partial H^*}{\partial y^*} = \rho^* c_p^* u^* T^* - \lambda^* \frac{\partial T^*}{\partial x^*} \tag{5}$$

and for the y^*-direction as:

$$-\frac{\partial H^*}{\partial x^*} = \rho^* c_p^* v^* T^* - \lambda^* \frac{\partial T^*}{\partial y^*} \tag{6}$$

Heat function describes how the fluid flow transports heat, and in an analogous fashion stream function portrays the transport of mass by the flow. Streamlines are derived from the stream function. A streamline is herein defined as a line of constant stream function. These lines are used in practice for the presentation of the field of a flowing fluid. The stream function satisfies the mass continuity equation for an incompressible flow. This function is defined mathematically for the x^*- and the y^*-directions in Cartesian coordinates as:

$$\frac{1}{\rho^*}\frac{\partial \psi^*}{\partial y^*} = u^*, \quad -\frac{1}{\rho^*}\frac{\partial \psi^*}{\partial x^*} = v^* \tag{7}$$

In addition to the above-mentioned equations, the equations for the temperature and pressure dependence on density, viscosity, thermal conductivity and specific heat capacity are also necessary. However, the pressure dependence of the fluid properties is very small and can be neglected by the pressure difference that occurs in natural convective flow (Thielemann, 1985). Several variable properties analyses for enclosure flow are available in the literature. In this work the temperature dependence of the variable properties is taken into account by expanding them into Taylor series fixed at a certain reference state. By neglecting terms with order higher than two, one obtains, e.g. for density (Gersten and Herwig, 1984):

$$\rho^*(T^*) = \rho_R + \left(\frac{\partial \rho^*}{\partial T^*}\right)_R (T^* - T_R) + \frac{1}{2}\left(\frac{\partial^2 \rho^*}{\partial T^{*2}}\right)_R (T^* - T_R)^2 + \cdots \tag{8}$$

The expression in equation (8) is cast into dimensionless form by making use of the normalization properties of the second kind defined as follows:

$$K_{\rho 1} = \left(\frac{T^*}{\rho^*}\frac{\partial \rho^*}{\partial T^*}\right)_R \tag{9}$$

$$K_{\rho 2} = \left(\frac{T^{*2}}{\rho^*}\frac{\partial^2 \rho^*}{\partial T^{*2}}\right)_R, \tag{10}$$

an expansion parameter:

$$\varepsilon = \frac{T_h - T_c}{T_R}, \tag{11}$$

and the dimensionless properties based on the reference temperature T_R:

$$\rho = \frac{\rho^*}{\rho_R}, \quad \mu = \frac{\mu^*}{\mu_R}, \quad \lambda = \frac{\lambda^*}{\lambda_R}, \quad c_p = \frac{c_p^*}{c_{p_R}} \tag{12}$$

By setting equations (9)-(12) in equation (8) results in:

$$\rho = \frac{\rho^*}{\rho_R} = 1 + \varepsilon K_{\rho 1} T + \frac{1}{2} K_{\rho 2} \varepsilon^2 T^2 \tag{13}$$

In a similar way, the expressions for the temperature dependence of other properties namely dynamic viscosity, thermal conductivity and specific heat capacity are obtained:

$$\mu = \frac{\mu^*}{\mu_R} = 1 + \varepsilon K_{\mu 1} T + \frac{1}{2} K_{\mu 2} \varepsilon^2 T^2 \tag{14}$$

$$\lambda = \frac{\lambda^*}{\lambda_R} = 1 + \varepsilon K_{\lambda 1} T + \frac{1}{2} K_{\lambda 2} \varepsilon^2 T^2 \tag{15}$$

$$c_p = \frac{c_p^*}{c_{p_R}} = 1 + \varepsilon K_{c_p 1} T + \frac{1}{2} K_{c_p 2} \varepsilon^2 T^2 \tag{16}$$

The reference temperature T_R is taken in this study as the arithmetic mean between the end wall temperatures:

$$T_R = \frac{T_c + T_h}{2} \tag{17}$$

The constants K in equations (13)-(16) are comparable with the Prandtl number and are dependent on the reference states (T_R, p_R). The values for these constants are presented in Table I for air, water and oil (shell voluta 919) according to Schlichting and Gersten (2000) and Gersten and Herwig (1984).

3. Method of analysis and the solution technique

The task now is to seek the solution of the governing equations (1)-(6) together with the temperature dependent fluid properties defined in equations (13)-(16). Till date, there is no close form solution of these equations. Theoretical solutions to the complete Navier-Stokes equations are only possible for limited cases, i.e. for creeping, potential and boundary layer flows. The advent of digital computer has, however, enabled an easy numerical solution of these equations. In this work, the model equations are solved numerically by using the finite difference method. This method has proved to be very efficient in the solution of partial differential equations of different forms.

For the numerical solutions of the model equations, they are foremost cast into dimensionless form. This becomes imperative for the sake of conveniences and to enable the generalisation of the governing equations so that they could be applied to a wide range of operating parameters. The following non-dimensional variables are thus introduced defined according to Hong (1992):

Fluid	Liquid sodium			Air			Water			Oil (Shell Voluta 919)		
T/K	473	673	873	293	473	773	273	293	343	273	293	343
Pr	0.0072	0.0056	0.0049	0.740	0.680	0.700	13.20	7.00	2.50	1303	412	81
$-\beta T = K_{\rho 1}$	−0.124	−0.189	−0.262	−1.000	−1.000	−1.000	0.010	−0.057	−0.205	−0.215	−0.234	−0.286
$K_{\mu 1}$	−0.918	−0.933	−0.941	0.733	0.695	0.626	−8.791	−7.142	−4.749	−19.970	−14.690	−8.403
$K_{\lambda 1}$	−0.310	−0.459	−0.618	0.906	0.820	0.747	1.008	0.825	0.493	−0.513	−0.166	−0.199
K_{cp1}	−0.149	−0.133	−0.055	−0.303	0.116	0.179	−0.188	−0.053	0.045	0.567	0.584	0.622
$K_{\rho 2}$	−0.006	−0.008	−0.008	2.000	2.000	2.000	−0.949	−0.907	−0.609	0.0	0.0	0.0
$K_{\mu 2}$	1.710	1.770	1.800	−0.385	−0.374	−0.350	113.36	78.362	38.61	512.42	291.03	105.575
$K_{\lambda 2}$	0.065	0.150	0.290	−0.380	−0.388	−0.382	−2.771	−2.597	−1.981	0.0	0.0	0.0
K_{cp2}	0.144	0.307	0.530	1.874	0.274	−0.174	2.619	1.496	0.262	0.0	0.0	0.0

Sources: Schlichting and Gersten (2000) and Gersten and Herwig (1984)

Table I.
The temperature-dependent physical properties of air, water and oil at reference pressure $p_R = 1$ bar

$$x = \frac{x^*}{l}, \quad y = \frac{y^*}{l}, \quad u = \frac{u^*}{(\mu_R/l\rho_R)}, \quad v = \frac{v^*}{(\mu_R/l\rho_R)} \quad T = \frac{(T^* - T_R)}{(T_h - T_c)},$$
$$\psi = \frac{\psi^*}{\mu_R/\rho_R}, \quad \omega = \frac{\omega^*}{(\mu_R/l^2\rho_R)}, \quad H = \frac{H^*}{\lambda_R(T_h - T_c)} \tag{18}$$

In the numerical solutions of the Navier-Stokes equations one possibility is to introduce stream function and vorticity. This possibility is a potent tool for solving especially two-dimensional flow equations and heat transfer problems. The method helps by taking care of the difficulty associated in the determination of pressure by eliminating the pressure derivative from the equations. The elimination of the pressure terms from equations (2) and (3) is done by cross-differentiating each term of the equations and then by subtracting the resulting equations one from the other. The resulting expression is simplified with the continuity equation (1) and the non-dimensional parameters defined in equation (18). The equation obtained is the dimensionless vorticity transport equation:

$$\begin{aligned}
&\frac{\partial(\rho u\omega)}{\partial x} + \frac{\partial(\rho v\omega)}{\partial y} + \frac{\partial\rho}{\partial x}\left(u\frac{\partial u}{\partial y} + v\frac{\partial v}{\partial y}\right) - \frac{\partial\rho}{\partial y}\left(u\frac{\partial u}{\partial x} + v\frac{\partial v}{\partial x}\right) \\
&\quad = -Ga\frac{\partial\rho}{\partial x} + \mu\left(\frac{\partial^2\omega}{\partial x^2} + \frac{\partial^2\omega}{\partial y^2}\right) \\
&\qquad + 2\left[\frac{\partial\mu}{\partial x}\left(\frac{\partial^2 v}{\partial x^2} + \frac{\partial^2 v}{\partial y^2}\right) - \frac{\partial\mu}{\partial y}\left(\frac{\partial^2 u}{\partial x^2} + \frac{\partial^2 u}{\partial y^2}\right) + \frac{\partial^2\mu}{\partial x\partial y}\left(\frac{\partial v}{\partial y} - \frac{\partial u}{\partial x}\right)\right] \\
&\qquad + \left(\frac{\partial^2\mu}{\partial x^2} - \frac{\partial^2\mu}{\partial y^2}\right)\left(\frac{\partial u}{\partial y} + \frac{\partial v}{\partial x}\right),
\end{aligned} \tag{19}$$

where ω is called the vorticity and is defined as:

$$\omega = \frac{\partial v}{\partial x} - \frac{\partial u}{\partial y} \tag{20}$$

By substituting equation (7) into equation (20) and reducing the resulting expression with the dimensionless variables defined in equation (18), the non-dimensional stream function equation is obtained:

$$-\omega = \frac{\partial}{\partial x}\left(\frac{1}{\rho}\frac{\partial\psi}{\partial x}\right) + \frac{\partial}{\partial y}\left(\frac{1}{\rho}\frac{\partial\psi}{\partial y}\right) \tag{21}$$

Equation (4) is simplified by using the nominalization parameters defined in equation (18) to derive the normalized energy transport equation:

$$\frac{\partial(\rho u T)}{\partial x} + \frac{\partial(\rho v T)}{\partial y} = \frac{1}{Pr}\left[\frac{\partial}{\partial x}\left(\lambda\frac{\partial T}{\partial x}\right) + \frac{\partial}{\partial y}\left(\lambda\frac{\partial T}{\partial y}\right)\right] \tag{22}$$

The heat function equation is derived from equations (5) and (6) by cross-differentiating each member of the equations, subtracting one from the other

and then by reducing the resulting expression with the nominalization parameters to give:

$$\frac{\partial^2 H}{\partial x^2}+\frac{\partial^2 H}{\partial y^2}=Pr(1+J)\left(\frac{\partial(\rho c_p uT)}{\partial y}-\frac{\partial(\rho c_p vT)}{\partial x}\right)+\frac{\partial}{\partial x}\left(\lambda\frac{\partial T}{\partial y}\right)-\frac{\partial}{\partial y}\left(\lambda\frac{\partial T}{\partial x}\right) \quad (23)$$

In the above equations Ga denotes the Galilei number defined in terms of the fluid properties and the cavity dimension as:

$$Ga=\frac{g\rho_{\mathrm{R}}^2 l^3}{\mu_{\mathrm{R}}^2}$$

Galilei number is related with the Grashof number Gr through the expression:

$$Gr=Ga\beta_{\mathrm{R}}(T_{\mathrm{h}}-T_{\mathrm{c}})$$

where β_{R} is the volumetric coefficient of thermal expansion. The product of Prandtl number $Pr=\upsilon/\alpha=c_{p_{\mathrm{R}}}\mu_{\mathrm{R}}/\lambda_{\mathrm{R}}$ and the Grashof number $Gr=gl^3\beta(T_{\mathrm{h}}-T_{\mathrm{c}})/\upsilon^2$ gives the Rayleigh number Ra, which is the most common dimensionless number in use in the study of natural convection. In equation (23) the variable J is defined as $J=T_{\mathrm{R}}/(T_{\mathrm{h}}-T_{\mathrm{c}})\geq 0$, which is the inverse of the expansion parameter.

The flow patterns, the energy trajectory and the energy transfer rate depend mainly on the imposed boundary conditions. So, to completely characterise the flow, boundary conditions must be given. The energy and the momentum transport in the investigated enclosure are subject to the following boundary conditions in non-dimensional form:

$$\begin{aligned} &u=v=0, \quad \frac{\partial T}{\partial y}=0, \quad \text{at } y=(0,1),\ 0\leq x\leq 1,\ \omega\neq 0\\ &u=v=0, \quad T=1 \text{ at } x=0,\ 0\leq y\leq 1,\ \omega\neq 0\\ &u=v=0, \quad T=0, \quad \text{at } x=1,\ 0\leq y\leq 1,\ \omega\neq 0 \end{aligned} \quad (24)$$

The vorticity at the boundary is not zero but it assumes a definite value. This value can be computed from the first derivative of velocity or the second derivative of the stream function (Roache, 1976):

$$\omega_w=-\frac{2(\psi_{w+1}-\psi_w)}{\rho_w\Delta n^2}, \quad (25)$$

where the subscripts w and $(w+1)$, respectively, represent the grid point on the wall and the first grid point away from the wall, and Δn is the perpendicular distance between the wall and the first grid point normal to the wall. The numerical simulation by using the vorticity boundary condition as spelt out by equation (25) is essentially more stable as, would be with the boundary condition by Chow and Tien (1978):

$$\omega_w=-\frac{8\psi_{w+1}-7\psi_w-\psi_{w+2}}{2\rho_w\Delta n^2} \quad (26)$$

The boundary conditions for heat function are derived directly from equations (5) and (6) which are the basic definitions of the function:

$$H = \int_0^y \left(-\frac{\partial T}{\partial x}\bigg|_{x=0} \right) \mathrm{d}y \text{ and } \frac{\partial H}{\partial x} = 0 \quad \text{at } x = 0 \text{ and } 1$$

$$H = 0 \text{ and } \frac{\partial H}{\partial y} = -\frac{\partial T}{\partial x} \quad \text{at } y = 0 \tag{27}$$

$$H = Nu \text{ and } \frac{\partial H}{\partial y} = -\frac{\partial T}{\partial x} \quad \text{at } y = 1$$

Nu in equation (27) depicts the Nusselt number, which is used to determine the effect of fluid flow on the heat transfer. The value of the Nusselt number is computed after the flow, the temperature and the energy fields had been determined. The overall conduction-reference Nusselt number is evaluated by computing the net heat transfer Q entering the system through the heated portion of the driving wall and dividing it by the heat transfer by conduction:

$$Nu = \frac{Q}{\lambda \Delta T} = -\frac{\lambda_{\mathrm{h}}}{\lambda_{\mathrm{R}}} \int_0^1 \left(\frac{\partial T}{\partial x} \right)_{x=0} \mathrm{d}y \tag{28}$$

In equation (28) λ is the thermal conductivity of the fluid in the enclosure.

The dimensionless governing equations (19)-(23) together with the boundary conditions defined in equations (24)-(27) were discretized by using the finite difference formulation. Details on this method can be found in the book from Tannehill *et al.* (1997). For the purpose of the discretization of the governing equations, the control surface was divided into M grid divisions of length Δx in the x-direction and N grid division of Δy in the y-direction.

Central difference scheme was used to discretize all but the convective non-linear terms of the governing equations. The central difference approximation is second order accurate, but it does not represent the physics of the convective transport correctly and also leads to instabilities. For the purpose of the discretization of the convective non-linear terms, the energy, vorticity transport and the heat function equations are foremost transformed into their conservative form. Upwind difference scheme is then used to discretize the convective non-linear terms of the equations. This scheme is more stable and leads to better convergence of the computation process. In upwind difference scheme the direction of the flow is considered. A high stability of the solution of the numerical computation is achieved by using the alternating-direct implicit, ADI method.

The discretization of the flow fields and the governing equations results in a number of simultaneous linear equations corresponding to the number of nodal points. The solution of the linear equations is done iteratively by employing the successive over relaxation method. This method enhances the rate of convergence. A generalized expression for the solution of the governing equations is:

$$\Phi_{i,j}^{n+1} = (1 - \Omega)\Phi_{i,j}^{n} + \Omega \left[A_{i,j}\Phi_{i+1,j}^{n} + B_{i,j}\Phi_{i-1,j}^{n+1} + C_{i,j}\Phi_{i,j+1}^{n} + D_{i,j}\Phi_{i,j-1}^{n+1} + E_{i,j} \right] \tag{29}$$

In the above equation, Φ stands for the temperature T, stream function ψ, vorticity ω or heat function H at every nodal point. The definitions of the functions A, B, C, D and

E depend on the equation being solved. The indices i and j determine the nodal point, n stands for the iteration's level, and Ω is called the relaxation factor. It was found out by numerical experiments and in close agreement with the results of Hong (1992) and Thielemann (1985) that for the solution of the energy transport equation a value of Ω in the range 0.8 and 1.2 is essential for numerical stability. For the stream function equation the value of Ω in the range 0.8 and 1.8 should be chosen, and the value of Ω between 0.01 and 0.5 for the vorticity transport and heat function equations. For any of theses primary variables a higher value of Ω is required for lower Rayleigh number and lower value of Ω for higher Rayleigh number.

At the beginning of numerical simulations, the initial values for temperature, stream function, vorticity, velocity components and the heat function at all the interior grid points are set to zero. The velocity components are obtained in dimensionless form from equation (7). The computation algorithm is such that the fluid thermal and transport properties are foremost-determined at all the inner nodal points. This is followed by the computation of temperature, vorticity, stream function and the heat function at all the inner nodes and boundaries. The iteration is carried out until the following convergence criterion is satisfied at every internal grid point:

$$\frac{\sum_{j=2}^{N}\sum_{i=2}^{M}\left|\Phi_{i,j}^{n+1}-\Phi_{i,j}^{n}\right|}{\sum_{j=2}^{N}\sum_{i=2}^{M}\left|\Phi_{i,j}^{n}\right|}\leq\delta \tag{30}$$

where Φ is the primary variable being tested, and n denotes the number of iteration steps. Equation (28) was integrated numerically using the Simpson rule after the final temperature field was obtained to compute the overall Nusselt number.

4. Discussion of numerically generated results

The results of the numerical analysis developed in this work are presented in the form of thermal and heat function fields, and in form of the heat function profiles for Prandtl number in the range 0.01 and 450 and Rayleigh number ranging from 10^3 to 10^6. A number of numerical computations were carried out to determine among others the accuracy and the stability of the results with the number of the grid points. The accuracy of the numerically generated results was found to depend strongly on the number of nodal points. With a grid system of 41×41 nodal points, the numerical results were found to agree closely with many benchmark results. The results were considered for square enclosures only.

In order to ascertain the validity of the code used in this work, preliminary runs were made for several test cases for Boussinesq-approximation's problem. Table II compares steady-state Nusselt number obtained using the developed code with those reported by Hong (1992). The comparison covers a large range of Rayleigh and Prandtl numbers. It can be seen from the table that for all Prandtl numbers at low Rayleigh number, i.e. $Ra = 10^3$, $Nu \approx 1$, depicting a *quasi*-pure conductive heat transfer. The conductive heat transfer rate as indicated by the Nusselt number increases with the increase in Prandtl and Rayleigh numbers. Comparison of the results of the present

simulations with that of Hongs shows a very close agreement in the value of Nusselt number computed with the deviation of order < 0.3 per cent. Further validation of the results done by comparing the present computed Nusselt numbers with the correlation from Thielemann (1985) and Merker and Mey (1987) shows a very good agreement. By monitoring the convergence criterion for all the fields during the running of the programme, it was observed that a slight numerical instability in computation set in when the Prandtl number is smaller than 0.001 and the Rayleigh number is high (e.g. of order $\geq 10^6$) due to turbulence in the flow.

The effects of the combined variables thermodynamic and transport fluid properties on the Nusselt number were also investigated. The computation is done for air with Prandtl number of 0.7 at a reference temperature of 773 K. The results as shown in Figure 2 reveal that the Nusselt number depends very strongly on the expansion parameter. An increase in this parameter leads to a corresponding increase in Nusselt number. These curves show that Nusselt number increase with

	Nusselt number, *Nu*					
	$Ra = 10^3$		$Ra = 10^5$		$Ra = 10^6$	
Pr	This work	Hong (1992)	This work	Hong (1992)	This work	Hong (1992)
0.01	1.05970	1.05190	2.60512	2.59570	4.90408	4.64310
0.10	1.11967	1.11510	3.88174	3.82780	7.48337	7.32690
0.70	1.13290	1.13320	4.62014	4.58850	9.37705	9.28300
1.00	1.13352	1.13410	4.71013	4.67780	9.57108	9.48510
7.00	1.13473	1.13610	4.86788	4.83750	9.93769	9.85130
10.0	1.13479	1.13620	4.87167	4.84130	9.94940	9.86180
100	1.13491	1.13640	4.87742	4.84670	9.96913	9.87810

Table II.
Comparison of the Nusselt number, *Nu* with the numerical results from Hong (1992)

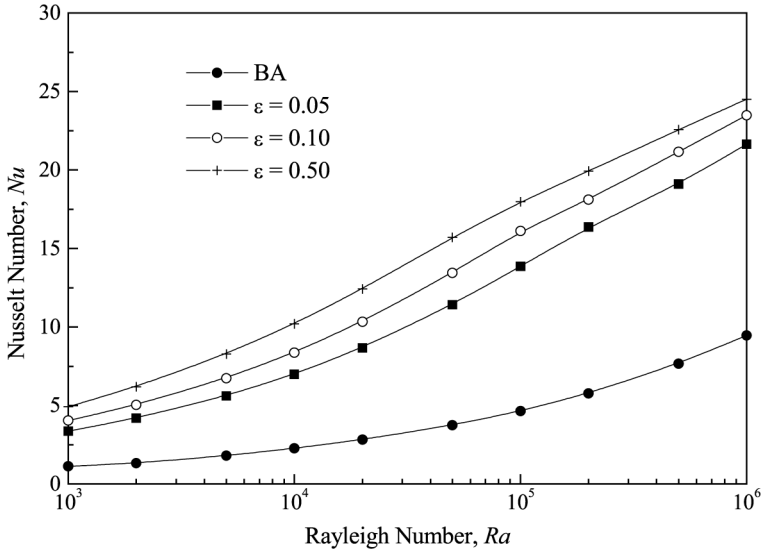

Figure 2.
Comparison of the convective heat transfers across a two-dimensional square enclosure for problem with Boussinesq-approximation and combined variable fluid properties

Rayleigh number. This result is consistent with the results of number of previous investigations (Inaba and Fukuda, 1984; Ivey and Hamblin, 1989; Lee, 1999). A comparison is drawn between the Nusselt number computed for Boussinesq-approximation's problem and that computed by allowing the variation of the fluid properties with temperature. It can be seen that the Nusselt number computed for Boussinesq-approximation's problem is smaller for all the range of Rayleigh number considered than those computed for the combined variable fluid properties. This signifies the fact that Boussinesq-approximation cannot be used to accurately simulate fluid flow at high temperature. It can also be seen that the Nusselt number increases with the expansion parameter. This is to be expected since an increase in the expansion parameter means that the temperature difference between the hot and the cold walls has increased. Zhong *et al.* (1985) stated that the BA should be adequate for $\varepsilon \leq 0.10$, where ε was defined as $\varepsilon = (T_h - T_c)/T_c$. The present results show that the expansion parameter should be far < 0.05 for the flow to satisfy the BA.

For visual interpretation of the results, the temperature and the heat function matrix were converted into isotherms and heatline plots, respectively. These are shown in Figure 3 for air with Prandtl number of 0.7 and Rayleigh number of 10^3. The computed temperature field for the Boussinesq-approximation (Figure 3(a)) compares favourably well with the results of previous investigations (Kimura and Bejan, 1983; Griebel *et al.*, 1998). At this Rayleigh number conductive heat transfer predominates. Thus the isotherms (Figure 3(a)) and heatlines (Figure 3(b)) are slightly influenced by convection. The heatlines and the isotherms computed for the same Rayleigh and Prandtl numbers when the combined variable fluid properties are considered are as reflected in Figure 3(c) and (d). These fields are seen to deviate strongly from those computed for BA. It can be seen in Figure 3(c) that the temperature gradient dT/dx near both cold and hot vertical walls is very high as compared with that of Figure 3(a). Consequently, the heatlines shown in Figure 3(d) deform very sharply than that of Figure 3(b). This probably explained the perceptible non-fulfilment of the normal boundary condition by the heat function on both vertical walls, although zero error in the software used to plot the field cannot be ruled out. This strong deviation can be justified by the fact that at the reference temperature in question ($T = 773$ K), the molecules of the fluid will be at very high random motion. The tempo of heat communication in the enclosure through convection will thus be very high. These results further buttress the fact that the state of the fluid in relation to temperature can only be reliably simulated when the effect of the variable fluid properties are considered.

To quantitatively estimate the degree of the effect of the variable fluid properties on heatlines, heat function both at the midplane ($x = 0.5$) and midheight ($y = 0.5$) is plotted against the transverse and longitudinal coordinates, respectively. These profiles are shown in Figures 4-8 for various flow conditions. Figure 4 is computed for $Pr = 0.7$ and $Ra = 10^3$ at a reference temperature of 773. The profiles for both BA and the combined VFP are presented on the same axes. The diagram shows that the heat function profiles along the midplane for the two cases (BA and VFP) start with a value of zero at $y = 0$. While the heat function for the BA increases steadily with the longitudinal coordinate, it foremost reduces for the VFP before rising. In the two cases, the values of the heat function at $y = 1$ correspond to their Nusselt numbers. The curve along the transverse coordinate has a *quasi*-parabolic profile, falling from a particular

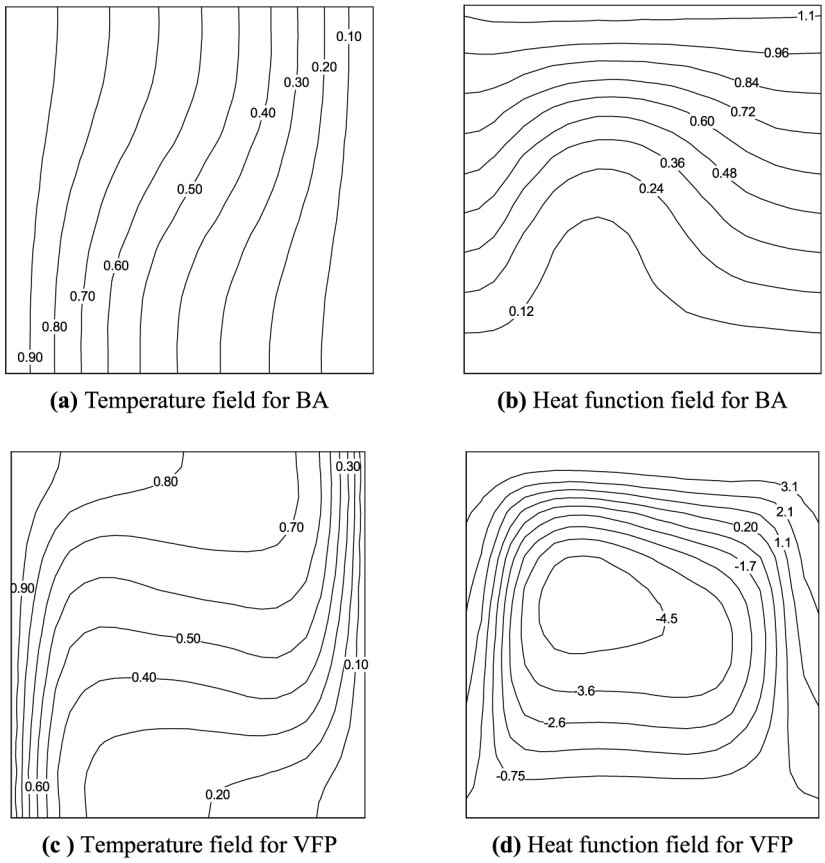

(a) Temperature field for BA

(b) Heat function field for BA

(c) Temperature field for VFP

(d) Heat function field for VFP

Figure 3.
The temperature and the heat function fields, respectively, for (a) and (b) Boussinesq-approximation, and (c) and (d) combined variable fluid properties in an air enclosed cavity at $T_R = 773\,K$ for $Ra = 10^3$, $Pr = 0.7$ and $\varepsilon = 0.1$

value at $x = 0$ to a minimum heat function at a point about $x = 0.5$ and rising back to the starting value at point $x = 1$. The curve for BA has a smaller gradient than that of VFP. This signifies a great effect of variable fluid properties on the heat function profiles.

An increase in the Rayleigh number results in changes in the gradient of the curves along the transverse and the longitudinal coordinates. The change, which becomes obvious when Figure 4 is compared with Figure 5, is the consequence of the increase in the flow buoyancy force. The overall effect of the variable fluid properties is to reduce the velocity in the wall region, but to increase it in the core region.

Figure 6 is shown to enable a comparison of the effects of the Prandtl number on the heat function profiles in the two coordinates. The curves are prepared at $Ra = 10^5$ for air with $Pr = 0.74$, water ($Pr = 7.0$) and shell oil ($Pr = 412$) at a reference temperature $T_R = 293\,K$, and liquid sodium ($Pr = 0.0074$) at $T_R = 473\,K$. From the heat function profiles for liquid sodium, it can be seen that the effect of convection on the fields is very weak. It should be noted that Prandtl number is a

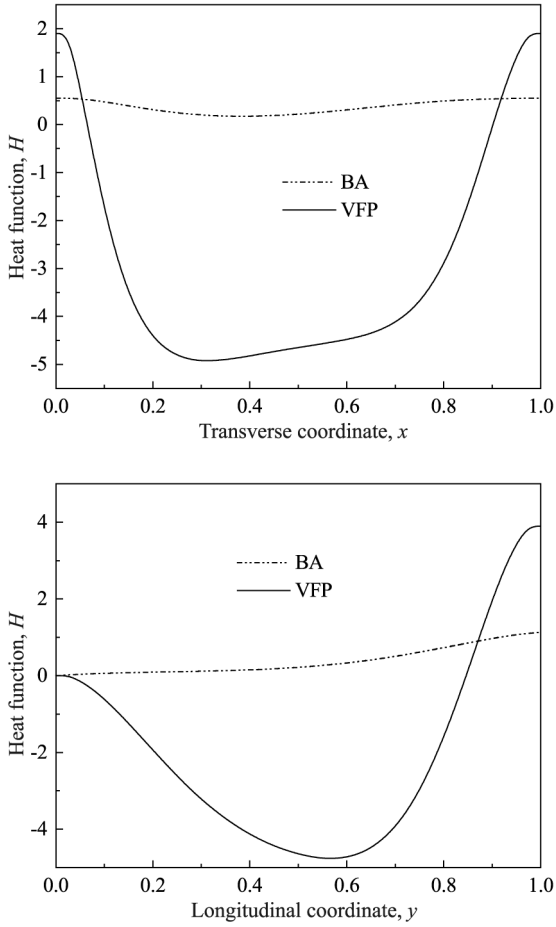

Figure 4.
The transverse and the longitudinal heat function profiles in a square enclosure filled with air at a reference temperature $T_R = 773\,K$ for $Ra = 10^3$, $Pr = 0.7$ and $\varepsilon = 0.1$

measure of the fluid material property, and thus varies from fluid to fluid. It is a measure of the relative importance of heat conduction and viscosity of fluid. This number is defined as the ratio of fluid momentum to thermal diffusivity. So $Pr \ll 1$ could result from very small momentum diffusivity (very weak convection) or very high thermal diffusivity. The effect of convection on heat function is appreciable for $Pr = 0.74$ resulting in high gradients of the profiles at both vertical walls, and small gradient in the inner space. For $Pr = 7$ and 412, the heat function curves collapse to a single curve near both vertical walls. In the inner space, the heat transfer rate for shell oil is higher than that for water. The difference in the heat transfer rate is due to the difference in the Prandtl number.

Figure 7 shows the curves of the heat function against the transverse and the longitudinal coordinates. The computation was done with water as the enclosed fluid at a reference temperature $T = 293$, $Ra = 10^3$ and $Pr = 7$. Other variable used in the

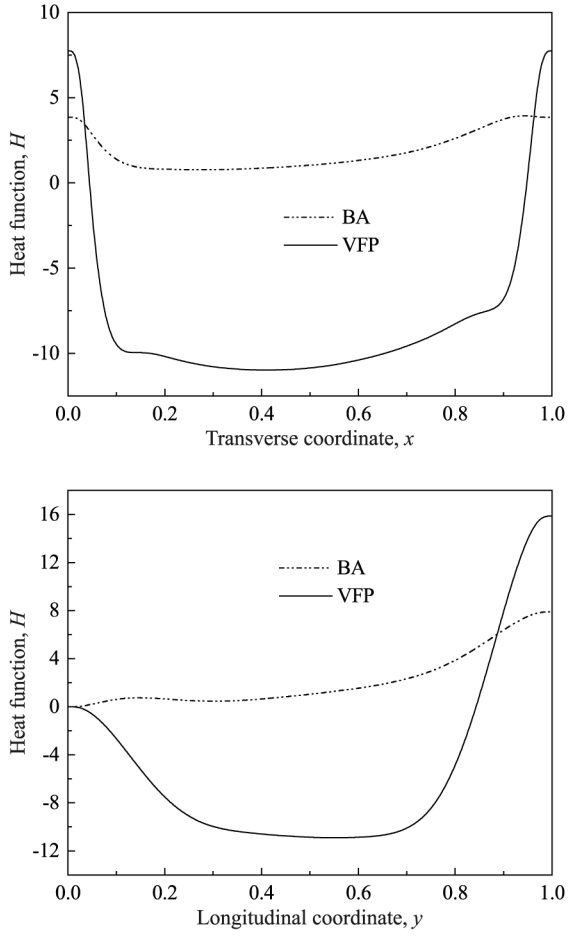

Figure 5.
The transverse and the longitudinal heat function profiles in a square enclosure filled with air at a reference temperature $T_R = 773\,K$ for $Ra = 10^5$, $Pr = 0.7$ and $\varepsilon = 0.1$

preparation of the curves is the expansion parameter $\varepsilon = 0.05$, 0.1 and 1.0. The profiles reveal that the heat function along the midplane and the midheight is appreciably influenced by changes in the expansion parameter. Comparing the curve for each of the expansion parameter with one another, it can be seen that $\varepsilon = 0.05$ has the least effect while $\varepsilon = 1.0$ has the greatest. The shape of the heat function curves along either coordinate change with the expansion parameter. The curve for $\varepsilon = 1.0$ along the transverse coordinate has a *quasi*-parabolic profile.

Each of the fluid properties was varied separately to quantitatively determine what the relative contributions of each should be when all were allowed to vary simultaneously. The analysis was done with air as the considered fluid at reference temperature $T = 773$, $Ra = 10^3$ and $Pr = 0.7$. Figure 8 shows that the heat function along the transverse coordinate is hardly influence by variable viscosity, thermal conductivity and specific heat capacity. The heat function curve for the variable

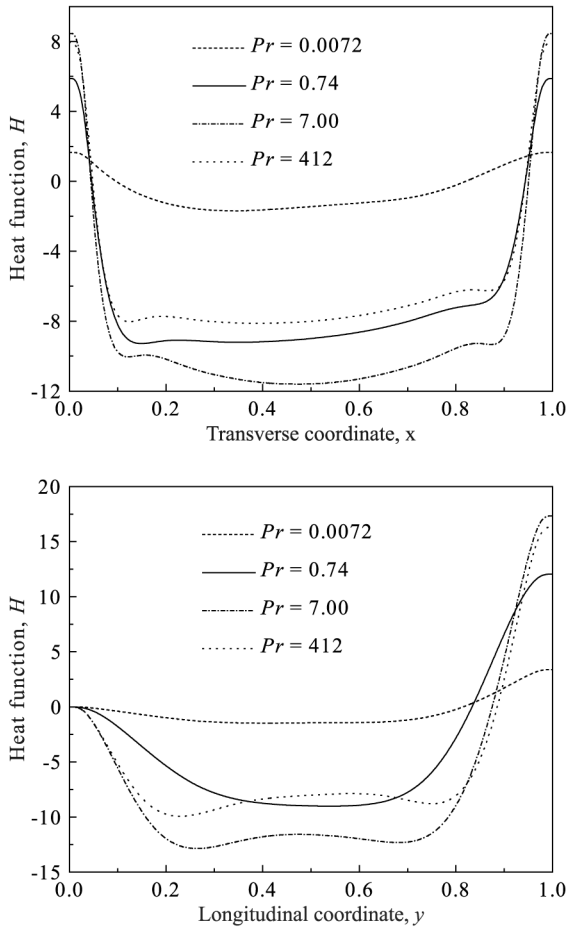

Figure 6.
Comparison of the effect of Prandtl number on the heat function profiles for $Ra = 10^5$ at a reference temperature $T_R = 293\,K$ and $\varepsilon = 0.1$

density has a parabolic profile showing a strong influence of the separate variable density. A comparison of the profiles for the transverse and the longitudinal coordinates reveals that an appreciable variation of the heat function occurs along the longitudinal coordinate. The curves reflect that the heat function for both variable specific heat capacity and viscosity varies linearly with equal magnitude along the coordinate. The values of heat function along the coordinate for variable thermal conductivity are slightly smaller. The profile also shows a strong effect of the variable density on the heat function along the longitudinal coordinate. The results, which are in close agreement with those of Mahony *et al.* (1986), are plausible because the convective flow itself is induced by variation in density with temperature changes. Besides, density appears in all the governing equations. Owing to the low velocity in laminar natural convection, variable viscosity is not expected to significantly influence the heat function profiles.

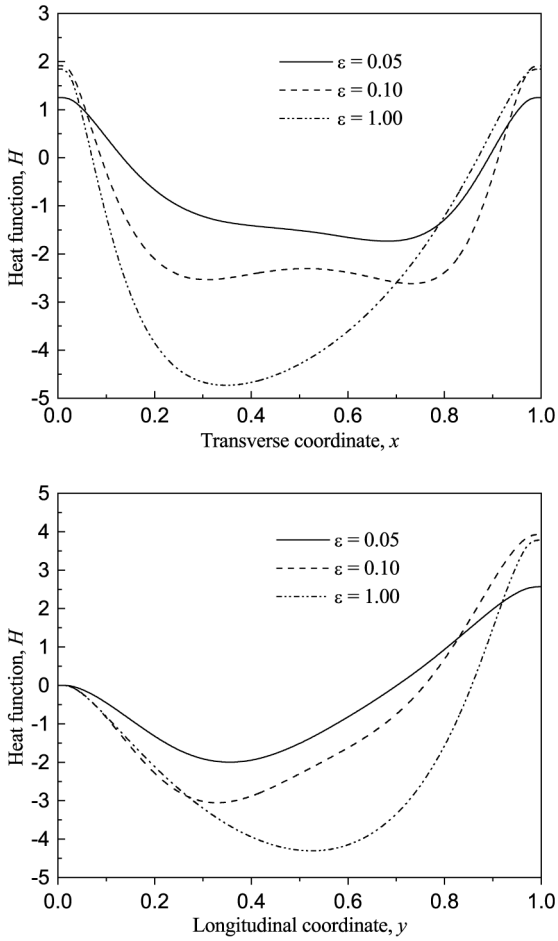

Figure 7.
The effects of the expansion parameter on the heat function profile in a water enclosed cavity at a reference temperature $T_R = 293\,K$, $Pr = 7.0$ and $Ra = 10^3$

5. Conclusions

Heat function formulation of the natural convective flow under the consideration of the temperature dependent density, viscosity and thermal conductivity and specific heat capacity was examined in this present work. The investigations were conducted numerically by using a finite-difference scheme. Upwind difference scheme is thereby used to discretize the convective non-linear terms of the equations. A high stability of the numerical computation is achieved by using the alternating-direct implicit, ADI method. The results of the work where compared where possible with those of other investigations, and agreements in such case were good. It was found that the heat transfer, the heat function fields and profile are dependent on the Rayleigh number, Prandtl number and the expansion parameter in a very complex way. Both the heat function and the temperature fields for VFP were seen to deviate from those of BA. Based on the results of this work, the following conclusions can be made:

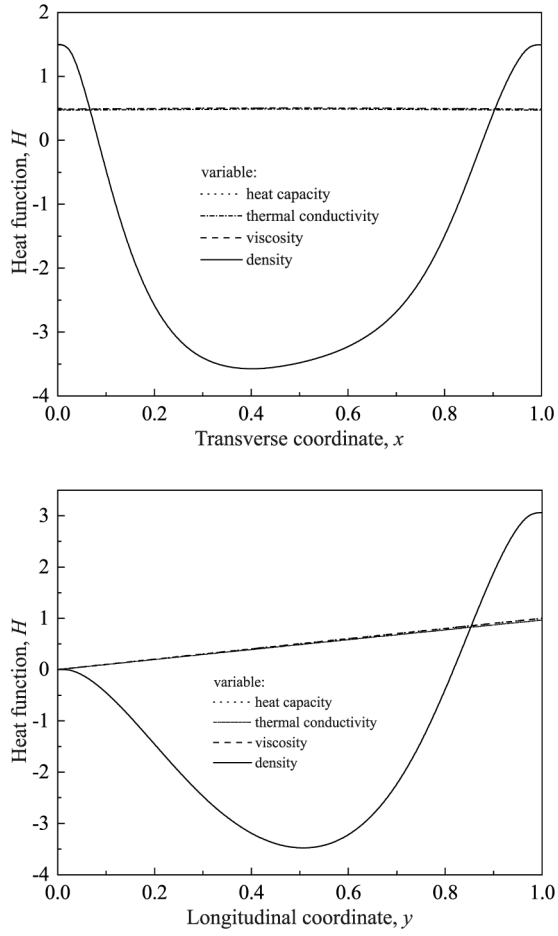

Figure 8.
Comparing the effects of variable fluid properties when separately considered on the heat function profile for $T_R = 773\,K$, $Pr = 0.7$, $Ra = 10^3$ and $\varepsilon = 0.1$

- the Boussinesq-approximation is not sufficient to simulate natural convective flow when the difference between T_h and T_c is high and close to the reference state temperature; and
- the effects of the other fluids properties other than density can be neglected in computation without significant loss of accuracy.

References

Bello-Ochende, F.L. (1986), "Analysis of heat transfer by free convection in tilted rectangular cavities using the energy-analogue of the stream function", *Int. J. Mech. Engrg Edu.*, Vol. 15 No. 2, pp. 91-8.

Bello-Ochende, F.L. (1988), "A heat function formulation for thermal convection in a square cavity", *Comp. Methods in Applied Mech. Engrg*, Vol. 68, pp. 141-9.

Chen, W.M., Shaw, H.J. and Huang, M.J. (1990), "Natural convection in partitioned enclosed spaces of solar collector", *Wärme- und Stoffübertragung*, Vol. 25, pp. 59-67.

Chow, L.C. and Tien, C.L. (1978), "An examination of four differencing schemes for some elliptic-type convection equations", *Num. Heat Transfer*, Vol. 1, pp. 87-100.

Cormack, D.E., Leal, L.G. and Imberger, D.E. (1974), "Natural convection in a shallow cavity with differentially heated end walls. Part 1. Asymptotic theory", *J. Fluid Mech.*, Vol. 65 No. 2, pp. 209-29.

De Souza, M., De Miranda, R.F. and Machado, H.A. (2003), "Natural convection in enclosures with variable fluid properties", *Int. J. Num. Method Heat Mass Flow*, Vol. 13 No. 8, pp. 1079-97.

De Vahl Davis, G. (1983), "Natural convection of air in a square cavity: a bench mark numerical solution", *Int. J. Num. Methods in Fluids*, Vol. 3, pp. 249-64.

Gersten, K. and Herwig, H. (1984), "Impuls- und Wärmeübertragung bei variablen Stoffwerten für die laminare Plattenströmung", *Wärme- und Stoffübertragung*, Vol. 18, pp. 25-35.

Griebel, M., Dornseifer, T. and Neunhoeffer, T. (1998), *Numerical Simulation in Fluid Dynamics: A Practical Introduction*, SIAM, Philadelphia, PA.

Hong, J. (1992), "Freie Konvektion in rechteckigen Hohlräumen und horizontalen Ringspalten unter Berücksichtigung variabler Stoffwerte", *VDI Fortschritt-Berichte*, Reihe 3: Verfahrenstechnik, Nr. 299.

Inaba, H. and Fukuda, T. (1984), "An experimental study of natural convection in an inclined rectangular cavity filled with water at its density extremum", *J. Heat Transfer*, Vol. 106, pp. 109-15.

Ivey, G.N. and Hamblin, P.F. (1989), "Convection near the temperature of maximum density for high Rayleigh number, low aspect ratio, rectangular cavities", *J. Heat Transfer*, Vol. 111, pp. 100-5.

Kelkar, K.M. and Patankar, S.V. (1990), "Numerical prediction of natural convection in square partitioned enclosures", *Num. Heat Transfer. Part A*, No. 17, pp. 269-85.

Kimura, S. and Bejan, A. (1983), "The 'Heatline' visualization of convective heat transfer", *J. Heat Transfer*, Vol. 105, pp. 916-19.

Lee, K.T. (1999), "Laminar natural convection heat and mass transfer in vertical rectangular ducts", *Int. J. Heat Mass Transfer*, Vol. 42, pp. 4523-34.

Mahony, D.N., Kumar, R. and Bishop, E.H. (1986), "Numerical investigation of variable property effects on laminar natural convection of gases between two horizontal isothermal concentric cylinders", *J. Heat Transfer*, Vol. 108, pp. 783-9.

Merker, G.P. and Mey, S.T. (1987), "Free convection in a shallow cavity with variable properties – 1. Newtonian Fluid", *Int. J. Heat Mass Transfer*, Vol. 30 No. 9, pp. 1825-32.

Miyamoto, M., Kuehn, T.H., Goldstein, R.J. and Katoh, Y. (1989), "Two-dimensional laminar natural convection heat transfer from a fully or partially open square cavity", *Num. Heat Transfer, Part A*, No. 15, pp. 411-30.

Mota, J.P.B., Esteves, I.A.A.C., Portugal, C.A.M., Esperança, J.M.S.S. and Saatdjian, E. (2000), "Natural convection heat transfer in horizontal eccentric elliptic annuli containing saturated porous media", *Int. J. Heat Mass Transfer*, Vol. 43, pp. 4367-79.

Roache, P.J. (1976), *Computation Fluid Dynamics*, Hermosa, Albuquerque, NM.

Schlichting, H. and Gersten, K. (2000), *Boundary Layer Theory*, 8th ed., Springer-Verlag, Berlin.

Tannehill, J.C., Anderson, D.A. and Pletcher, R.H. (1997), *Computational Fluid Mechanics and Heat Transfer*, 2nd ed., Taylor & Francis Publishers, New York, NY.

Thielemann, M. (1985), *Berechnung der freien Konvektion in Hohlräumen mit quadratischem Querschnitt unter Berücksichtigung Temperaturabhängiger Stoffwerte*, VDI Verlag, Düsseldorf.

Zhong, Z.Y., Yang, K.T. and Lioyd, J.R. (1985), "Variable properties effects on laminar natural convection in a square enclosure", *J. Heat Transfer*, Vol. 107, pp. 133-8.